Submitted: 17 February, 2023 Accepted: 25 March, 2023 Published: 15 December, 2023 DOI:10.22514/ejgo.2023.096

ORIGINAL RESEARCH

European Journal of Gynaecological Oncology

Construction of a ferroptosis-related lncRNA signature for predicting prognosis, immune response and drug sensitivity in cervical squamous cell carcinoma and endocervical adenocarcinoma

Tingting Gu[1,†], Caihong Xu[2,†], Jing Chen[2], Bin Wan[2], Wei Wang[3,*], Jun Shi[1,4,*]

[1]Department of Obstetrics and Gynecology, Affiliated Hospital of Nanjing University of Chinese Medicine, Taicang Hospital of Traditional Chinese Medicine, 215400 Taicang, Jiangsu, China
[2]Department of Obstetrics and Gynecology, Nanjing Tongren Hospital, School of Medicine, Southeast University, 211102 Nanjing, Jiangsu, China
[3]Department of Clinical Laboratory, Lianshui County People's Hospital, 223400 Huai'an, Jiangsu, China
[4]Department of Clinical Laboratory, Affiliated Hospital of Nanjing University of Chinese Medicine, Taicang Hospital of Traditional Chinese Medicine, 215400 Taicang, Jiangsu, China

***Correspondence**
sj1987517@163.com
(Jun Shi);
wangwei_shzu@163.com
(Wei Wang)

† These authors contributed equally.

Abstract

Ferroptosis, a recently identified cell death mode, has been shown to play critical roles in several malignant tumors. Long non-coding RNAs (lncRNAs) have been reported to modulate ferroptosis, thereby affecting the growth and prognosis of cancers. However, the association between lncRNA and ferroptosis in cervical squamous cell carcinoma and endocervical adenocarcinoma (CESC) remains unclear. The aim of this study was to identify ferroptosis-related lncRNAs (FRLs) associated with CESC prognosis and investigate their interaction with tumor immune response. R software and Perl were used to screen for aberrant expressed FRLs associated with CESC patient prognosis from The Cancer Genome Atlas (TCGA) database, including *AP003774.2*, *SOX21* antisense divergent transcript 1 (*SOX21-AS1*), myocardial infarction associated transcript (*MIAT*), *RUSC1* antisense RNA 1 (*RUSC1-AS1*), *AC004847.1*, *AC009097.2*, *MIR100* host gene (*MIR100HG*), *AC083799.1*, long intergenic non-protein coding RNA 958 (*LINC00958*), *AC009065.8* and *AC131159.1*. A risk score was calculated for each CESC patient individual according to the expression levels of 11 FRLs, based on which a prognostic model was built. Kaplan-Meier (K-M) survival curve analysis and Receiver Operating Characteristic (ROC) curve assessment were conducted to determine the predictive accuracy of the prognostic model. Lastly, the R software and CIBERSORT were employed to examine the differences in immune cell infiltration, immune checkpoint and drug sensitivity between the two subgroups. The 11 FRLs were used to construct a prognostic model that classified CESC patients into a high- or low-risk group. The FRL-based model was found to outperform traditional clinicopathological features in predicting CESC patient survival. Significant variations existed across subgroups in immune cell infiltration, immunological function, overall survival (OS), and inhibitory concentrations (IC50 values). Our findings provide novel insights into the role of FRLs in CESC and present a personalized predictive tool for determining patient prognosis, immune response and drug sensitivity.

Keywords

Ferroptosis; Immune cell infiltrate; Drug sensitivity; Biomarkers; LncRNA; Survival analysis; Cervical squamous cell carcinoma and endocervical adenocarcinoma

1. Introduction

CESC is responsible for approximately 604,100 new cases and more than 341,800 mortality annually, making it one of the most prevalent cancers globally [1, 2]. Despite the rapid advancement of emerging therapies such as targeted molecular treatment and immunotherapy, the 5-year survival rate for individuals with recurrent or metastatic CESC remains poor, at only 16.8%. Although the Tumor-Node-Metastasis (TNM) classification is the main staging system used to classify CESC and predict patients' outcomes, the prediction results remain limited. Therefore, identifying novel tumor markers that could complement or outperform the currently used TNM classification remains a focus in cancer diagnosis and treatment, especially for identifying respondents to immunotherapy and predicting CESC patient prognosis.

Recently, there has been increasing focus on the function of cell ferroptosis in tumor progression. Unlike apoptosis, necrosis and autophagy, ferroptosis is mediated by reactive oxygen species (ROS) and appears in cells as aberrant iron metabolism and lipid peroxidation [3–5]. A combination of drugs that target ferroptosis may substantially improve treatment outcomes, as ferroptosis has been shown to affect the

effectiveness of radiotherapy, chemotherapy and immunotherapy [6–8]. Although ferroptosis has been proven to significantly affect cancer development, apoptosis and treatment resistance in various tumors [9–11], only a few therapeutic targets connected to ferroptosis in CESC have been identified [12–14]. Consequently, screening ferroptosis-related genes (FRG) in TCGA-CESC might be crucial to improve the diagnosis, therapeutics and survival prediction of CESC patients.

Long non-coding RNAs (lncRNAs) are a subclass of ncRNAs that are 200 to 10,000 nucleotides long but do not encode proteins [15, 16]. Many investigations have shown that lncRNAs can influence tumor biological activities such as proliferation, apoptosis, invasion and metastasis through the regulation of gene expression [17–20]. Additionally, many investigations have revealed that lncRNA modulates the ferroptosis process in tumors. Zhang *et al*. [21] found that abnormally expressed hepatocellular carcinoma ferroptosis associative lncRNA (HEPFAL) in hepatocellular carcinoma accelerated solute carrier family 7 member 11 (SLC7A11) ubiquitination, reduced SLC7A11 protein stability and expression and promoted the ferroptosis process in hepatocellular cancer. Zhang *et al*. [22] discovered that the transcription factor p53 facilitated the expression of lncRNA nuclear paraspeckle assembly transcript 1 (NEAT1) in hepatocellular carcinoma and competed with myo-inositol oxygenase (MIOX) 3′ untranslated regions (3′ UTR) to bind miR-362-3p. Additionally, MIOX overexpression is reported to enhance ferroptosis in hepatocellular cancer. However, there have been no investigations on ferroptosis-related lncRNAs (FRLs) in CESC. Therefore, identifying FRLs related to the prognostic prediction of CESC might be significant.

Although the aberrant lncRNA expression and abnormal ferroptosis activity in tumor cells have been directly linked to tumor growth, their relationships and functions in CESC remain unclear. In this study, we utilized the R and Perl software to obtain RNA sequencing (RNA-seq) and clinicopathological data from the TCGA-CESC, identified 11 FRLs related to CESC prognosis, and constructed predictive models. Then, the FRLs pathway in CESC was further evaluated using gene set enrichment analysis (GSEA) and immune infiltration assessment, which served as a guide for CESC immunotherapy and prognosis prediction.

2. Materials and methods

2.1 Data retrieving

The RNA-seq data and clinical features of 309 CESC samples, comprising 306 tumor specimens and three healthy samples, were retrieved from The Cancer Genome Atlas (TCGA) website (https://portal.gdc.cancer.gov/). Perl was used to collect RNA data and classify them as lncRNAs and mRNA.

2.2 Ferroptosis-related lncRNAs identification

Ferroptosis-related genes (FRGs), which include 150 drivers, 109 inhibitors and 123 biomarkers, were obtained from the FerrDb website (http://www.zhounan.org/ferrdb/). FRGand lncRNAs were differentially expressed in CESC and healthy cervical tissues (log2 Fold Change (log2|FC|) ≥ 1 and False Discovery Rate (FDR) ≤ 0.05) by differential expression analysis. Then, utilizing correlation and co-expression assessment (coefficient ≥ 0.4 and p-value ≤ 0.001), ferroptosis-related lncRNAs were identified.

2.3 Construction of the lncRNA-gene co-expression network

First, the R software was used to filter FRLs and FRGs depending on the filtering requirements of correlation coefficient ≥ 0.4 and p-value ≤ 0.001. The co-expression of FRG and lncRNAs was examined using Perl in conjunction with the risk score for each individual. Then, the Cytoscape program was used to display the co-expressed FRG and lncRNAs.

2.4 Constructing and validating an FRL predictive model

First, the expression levels of lncRNAs and mRNAs in each sample were determined using Perl annotation of the RNA-seq data from CESC patients obtained from the TCGA database. The aberrant FRLs expression in CESC tumor tissues was investigated using differential expression, correlation and co-expression analyses. Multivariate proportional risk regression models were constructed using the least absolute shrinkage and selection operator (LASSO) tool. The risk score formula was then used to compute each TCGA-CESC subject's risk value. Individuals with TCGA-CESC were classified into two groups, namely a high- or low-risk group, by comparing each patient's risk score to the median score of the TCGA cohort. TCGA database was utilized to acquire the clinical information for subjects with CESC. The R tools (R x64 4.1.3, Lucent Technologies, Murray Hill, New Jersey, USA) "survival" and "survminer" were used to plot the Kaplan-Meier overall survival curve. Clinical indicators and risk scores were examined using univariate and multivariate Cox regressions to discover whether they were independent predictive variables for overall survival (OS). The prediction precision of the FRL-based predictive model was assessed by drawing ROC curves using the R program.

2.5 Functional enrichment analysis

First, data from TCGA-CESC patients were downloaded to determine the aberrant expression of FRG in CESC tumor tissues. Using the "clusterProfiler" tool of R software, Gene Ontology (GO) and Kyoto Encyclopedia of Genes and Genomes (KEGG) enrichment analysis of FRG was conducted to discover the biological process and signaling pathways associated with aberrant expression of FRG. CESC patients were classified into a high- or low-risk group utilizing a risk score equation. The molecular and biological variations between the two groups were examined using Perl and GSEA packages.

2.6 Differential analysis of m6A-related genes, immune characteristics and drug sensitivity

The developed prognostic model examined variations in immune cell infiltration, immunological performance, immune

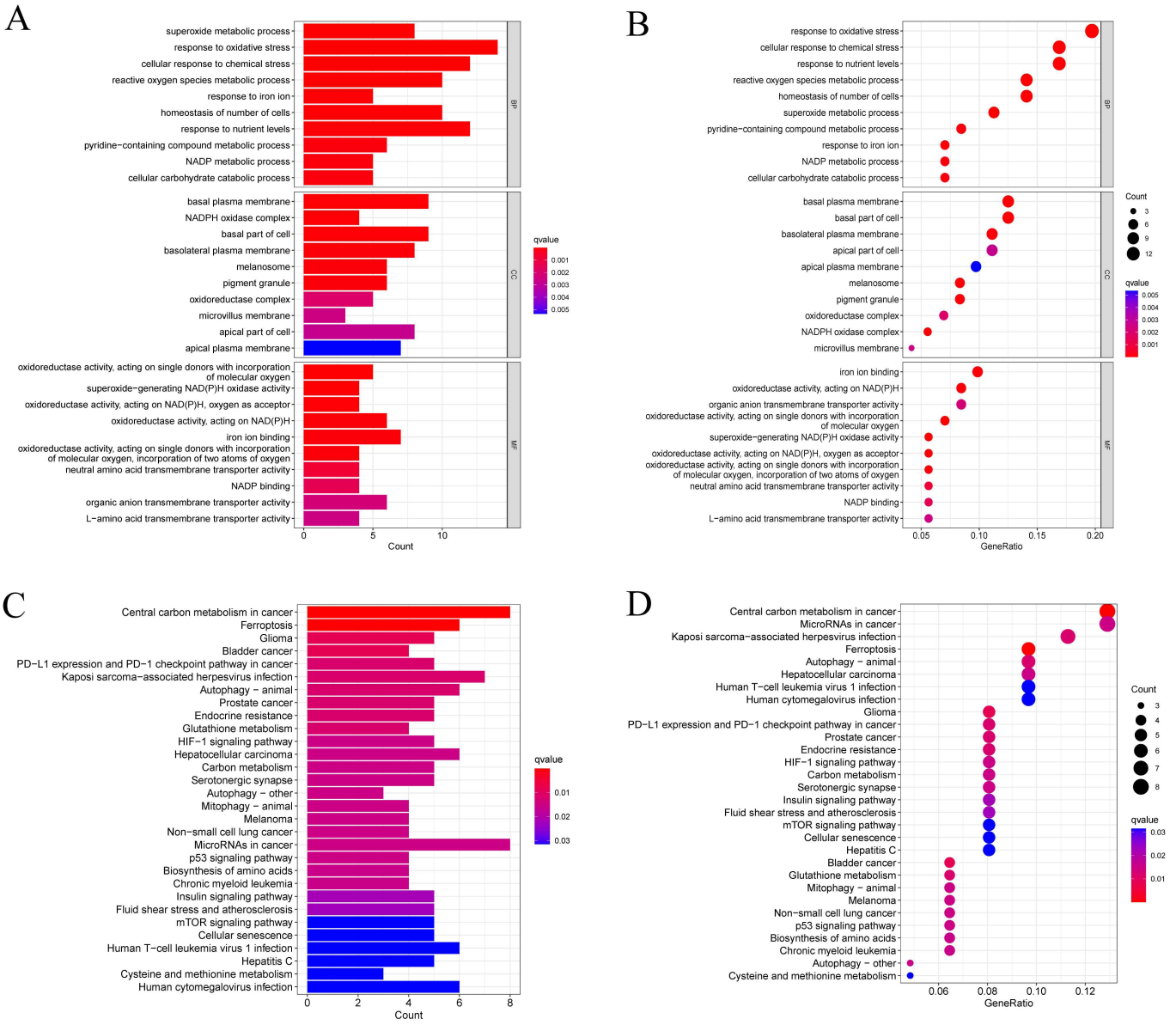

FIGURE 1. GO and KEGG enrichment analyses exploring the biological functions and signaling pathways involved in the abnormal expression of FRGs in CESC. (A,B) show significant GO functional items' bar and bubble plots; (C,D) show the bar and bubble plot of significant KEGG functional items. BP: biological process; CC: cellular component; MF: molecular function.

checkpoint, and m6A-associated genes. R software, e1071 Package, preprocessCore and limma were utilized to compare the variations in immune cell infiltrate between both groups. Immune function differences in the high- and low-risk groups were examined utilizing limma, Gene Set Enrichment Analysis Base (GSEABase), Gene Set Variation Analysis (GSVA), ggpubr, and reshape2. The limma, reshape2, ggplot2, pRRophetic and ggpubr packages were also used to investigate changes in immunological checkpoints, m6A-related genes and drug sensitivity across the two studied groups.

2.7 Statistical analysis

All statistical analyses were conducted utilizing the R program and its related packages. p values ≤ 0.05 were considered statistically significant.

3. Results

3.1 Identifying differentially expressed FRG and lncRNAs in CESC

We obtained 306 CESC and three normal cervical tissue samples from the TCGA database, and 19,895 mRNAs and 16,773 lncRNAs were retrieved. We downloaded 382 FRGs from the FerrDb database (http://www.zhounan.org/ferrdb/), comprising 150 Drivers, 109 inhibitors and 123 biomarkers (**Supplementary Table 1**). FRGs expression levels in cancerous and healthy tissues were determined, and their association with ferroptosis was evaluated. Using the parameters correlation coefficient $\geq$0.4 and p-values $\leq$ 0.0011, 201 FRGs were identified. From them, 72 FRGs and 271 FRLS were found to be differentially expressed between healthy cervical tissues and CESC, based on the log2|FC| $\geq$ 1 and FDR $\leq$0.05 filter

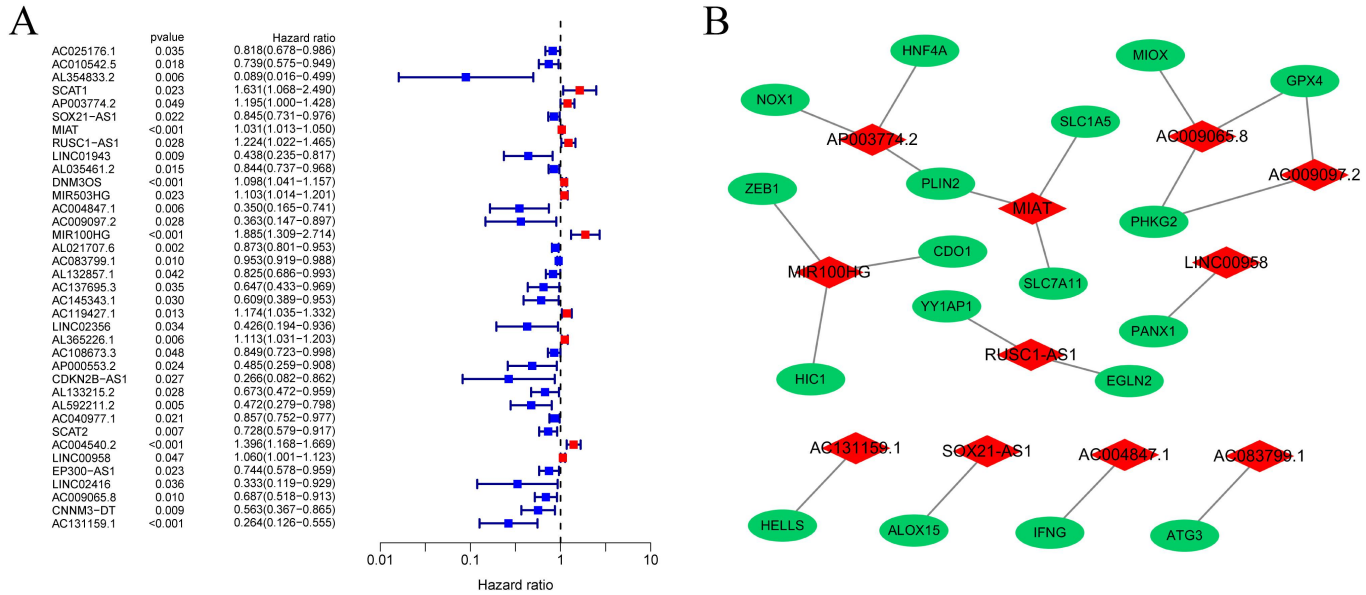

FIGURE 2. Identification of FRLs associated with CESC prognosis. (A) Forest plot of ferroptosis-related prognostic lncRNAs in TCGA-CESC. (B) Co-expression plots of FRLs and FRGs in a predictive model.

TABLE 1. The coefficient of the predictive model formula and the expression of 11 FRLs in CESC.

LncRNA	Expression In CESC	*p* Value	Risk model coefficient	Hazard ratio
AP003774.2	Up	0.0083	0.2052	1.195 (1.000−1.428)
SOX21-AS1	Up	0.0145	−0.1456	0.845 (0.731−0.976)
MIAT	Up	0.0067	0.0287	1.031 (1.013−1.050)
RUSC1-AS1	Up	0.0130	0.3694	1.224 (1.022−1.465)
AC004847.1	Up	0.0167	−1.5267	0.350 (0.165−0.741)
AC009097.2	Up	0.0041	−1.2465	0.363 (0.147−0.897)
MIR100HG	Down	0.0042	0.6836	1.885 (1.309−2.714)
AC083799.1	Up	0.0058	−0.0359	0.953 (0.919−0.988)
LINC00958	Up	0.0066	0.07136	1.060 (1.001−1.123)
AC009065.8	Up	0.0055	−0.2848	0.687 (0.518−0.913)
AC131159.1	Up	0.0053	−0.9980	0.264 (0.126−0.555)

CESC: cervical squamous cell carcinoma; SOX21-AS1: SOX21 antisense divergent transcript 1; MIAT: myocardial infarction associated transcript; RUSC1-AS1: RUSC1 antisense RNA 1; MIR100HG: MIR100 host gene; LINC00958: long intergenic non-protein coding RNA 958.

parameters (**Supplementary Tables 2,3**).

3.2 GO and KEGG enrichment analyses of differentially expressed FRGs in CESC

GO and KEGG analyses were performed to identify the biological roles and signaling pathways involved in differentially expressed FRGs. The GO analysis outcomes demonstrate that most differentially expressed genes were related to iron ions, oxidative stress, reactive oxygen species metabolism and iron ion binding (Fig. 1A,B). The KEGG analysis outcomes illustrate that most differentially expressed genes were primarily enriched in the Ferroptosis pathway, Programmed cell death 1 ligand 1 (PD-L1) expression, and Programmed cell death 1 (PD-1) checkpoint mechanism in malignancy, Kaposi sarcoma-associated herpesvirus infection pathway (Fig. 1C,D).

3.3 Identification of prognosis-related FRLs in CESC

The prognostic significance of these FRLs was assessed using Cox univariate regression using the TCGA CESC patients' survival data. We found that 37 FRLs were related to the prognosis of CESC patients (Fig. 2A). To further investigate the association between these FRLs and FRGs, a lncRNA-gene co-expression network was built, and 11 FRLs were discovered to be closely associated with FRGs which included *AP003774.2*, *SOX21-AS1*, *MIAT*, *RUSC1-AS1*, *AC004847.1*, *AC009097.2*, *MIR100HG*, *AC083799.1*, *LINC00958*, *AC009065.8* and *AC131159.1* (Fig. 2B).

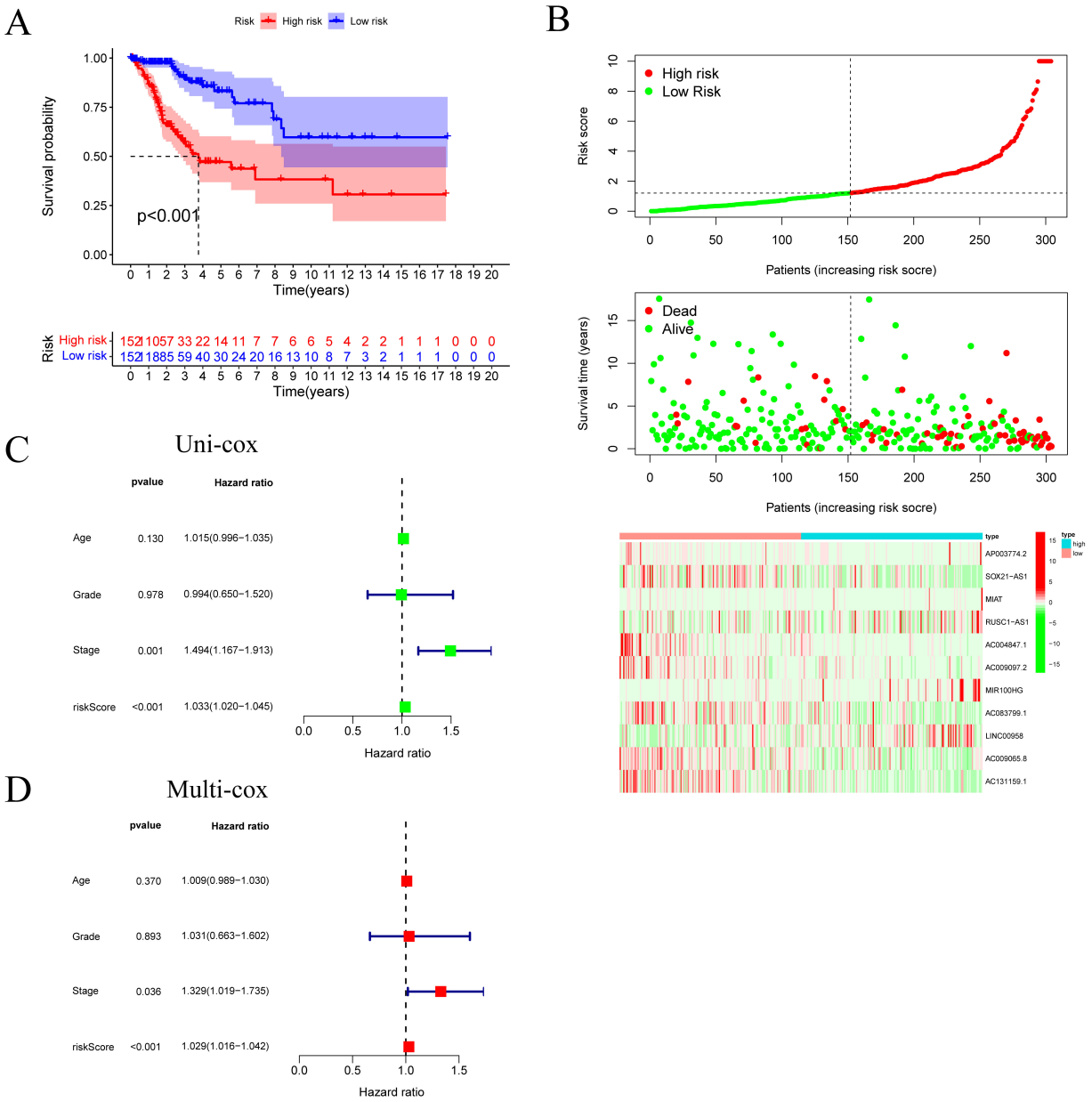

FIGURE 3. Developing and validating the prognostic model. (A) Kaplan-Meier curves showing the OS CESC patients from the high- and low-risk group; (B) Heatmap illustrating the expression of FRLs in groups at elevated and high risk; (C,D) Univariate and multivariate Cox regression analyses were performed to identify independent predictive variables. Uni-cox: Univariate Cox regression analysis; Multi-cox: Multivariate Cox analysis.

3.4 Constructing a predictive model in the TCGA cohort

Multivariate proportional risk regression models were built using the LASSO tool using the 11 FRLs (Table 1). Each CESC individual in the TCGA-CESC received a risk score for this model utilizing the following equation: Risk Score = *AP003774.2* × 0.2052 + *SOX21-AS1* × (−0.1456) + *MIAT* × 0.0287 + *RUSC1-AS1* × 0.3694 + *AC004847.1* × (−1.5267) + *AC009097.2* × (−1.2465) + *MIR100HG* × 0.6836 + *AC083799.1* × (−0.0359) + *LINC00958* × 0.07136 + *AC009065.8* × (−0.2848) + *AC131159.1* × (−0.9980). Of note, the lncRNAs shown here indicate their degree of expression in the TCGA database. The TCGA-CESC individuals were categorized into high- and low-risk groups by comparing their risk score with the median score of TCGA-CESC. The results showed that the OS rate of CESC patients in the high-risk group was lower than the low-risk group, according to Kaplan Meier analysis with log-rank testing ($p < 0.001$) (Fig. 3A). Based on the distribution of risk scores and OS, we observed that most deaths mainly occurred in the high-risk group. The candidate FRLs expression heatmap showed that eight lncRNAs (*AP003774.2*, *SOX21-AS1*, *MIAT*, *AC004847.1*, *AC009097.2*, *AC083799.1*, *AC009065.8* and *AC131159.1*) were primarily allocated into the low-risk group, and three lncRNAs (*RUSC1-AS1*, *MIR100HG* and *LINC00958*) in the high-risk group (Fig. 3B).

Univariate and multivariate Cox regression analyses were performed to identify independent parameters associated

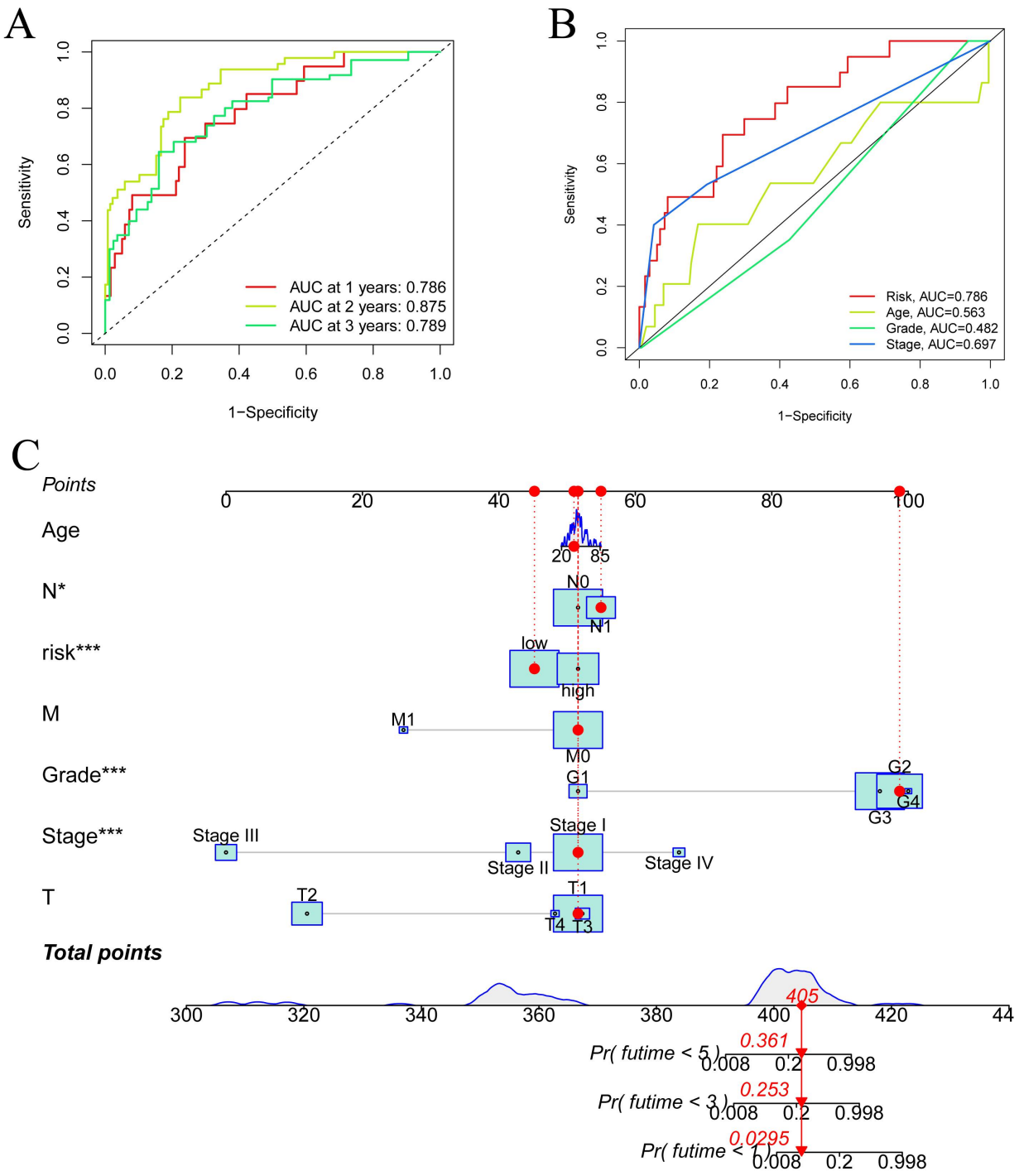

FIGURE 4. Validating the predictive model. (A) ROC curve showing the potential of predictive models based on FRLs in estimating 1-, 2- and 3-year OS; (B) AUC of ROC curves in assessing the predictive accuracy of the constructed model based on FRLs and other prognostic factors; (C) Nomogram for estimating the 1-, 3- and 5-OS rate of CESC patients. AUC: area under the curve; Pr: probability.

with patients' OS, based on which riskScore and Stage were identified as the independent prognostic variables in CESC (Fig. 3C,D). The time-dependent ROC analyses showed that the risk scores model's area under the curve (AUC) were 0.786, 0.875 and 0.789 at 1, 2 and 3 years, respectively (Fig. 4A). The AUC of the ROC curve constructed by FRLs was higher than that of the ROC curve created by other clinicopathological factors (Fig. 4B). The column charts anticipate the possibility of 1-, 3- and 5-year survival for these individuals using the scores of many involved parameters to improve the potential clinical applicability of the lncRNA-based signature (Fig. 4C). Analysis of the clinicopathological factors, including Age, Grade, Tumor Stage, and TNM staging, between the two risk groups showed that patients from the high-risk group had more advanced T stage than those in the low-risk group (Fig. 5).

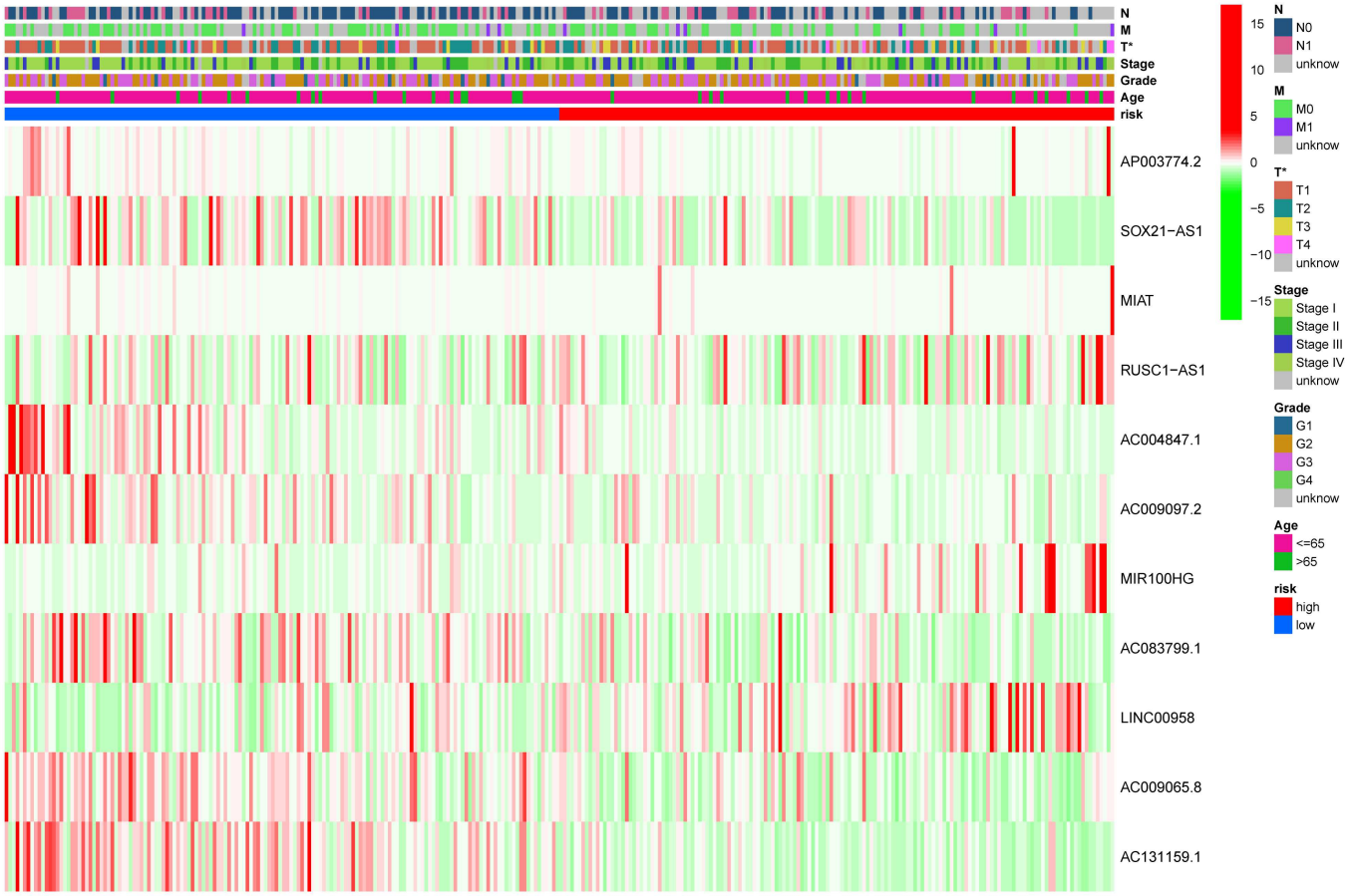

FIGURE 5. The heatmap shows variations in clinicopathological features between two risk subgroups.

3.5 GSEA pathway enrichment analysis

The different biological functions and signaling pathways between the two risk groups were investigated using the GSEA assessment. The results indicated that the high-risk group was primarily related to the transforming growth factor β (TGF-β) signaling pathway, modulation of the actin cytoskeleton, cancer-related pathways, and extracellular matrix (ECM) receptor interaction. The low-risk group was primarily involved in DNA replication, oxidative phosphorylation, primary immunodeficiency, and regulation of autophagy (Fig. 6).

3.6 Immune-related analysis of CESC patients

To examine the correlation between predictive models and anti-tumor immunology, differential analysis on immune cells, immunological activity, and immunotherapy concerning the predictive models of patients with CESC were conducted using the R program. The R software was used to recognize immune cell infiltration in TCGA-CESC individuals and create heatmaps for visualizing the differences (Fig. 7). The graph shows the ratio of each type of immune cell in the two studied groups (Fig. 8A,B). Various immune cells were more enriched in the low-risk group than in the high-risk group, including T cells CD4 memory activated, T cell CD8+, Macrophages M0, and Mast cells activated. Significant variations in immune function scores such as APC co-inhibition, checkpoint, HLA, inflammation-promoting, T cell co-inhibition and T cell co-stimulation between the two investigated groups were observed (Fig. 8C).

Next, we evaluated the immune checkpoint gene expression levels in the high- and low-risk groups. Of the 25 genes that showed differential expression between the two groups, 23 were substantially expressed in the low-risk group (Fig. 8D). Furthermore, m6A-related genes zinc finger CCCH-type containing 13 (*ZC3H13*), fragile X messenger ribonucleoprotein 1 (*FMR1*), leucine rich pentatricopeptide repeat containing (*LRPPRC*), YTH N6-methyladenosine RNA binding protein C1 (*YTHDC1*) and YTH N6-methyladenosine RNA binding protein F3 (*YTHDF3*) were found to be differently expressed between the two groups in the CESC prognostic model (Fig. 8E). Kaplan-Meier survival assessment revealed that differential expression of immune cells in the prognostic model was related to the OS of CESC patients (Fig. 8F). The results of drug sensitivity analysis revealed variations in IC50 values of several drugs between the high- and low-risk group (Fig. 9), implying that this prognostic model could also offer new insights into drug therapy for CESC patients.

4. Discussion

CESC is a highly incident cancer globally, and its recurrence and metastasis present significant challenges in CESC therapy [23, 24]. The pathogenesis of CESC involves a complicated and multifactorial, the human papillomavirus (*HPV*)

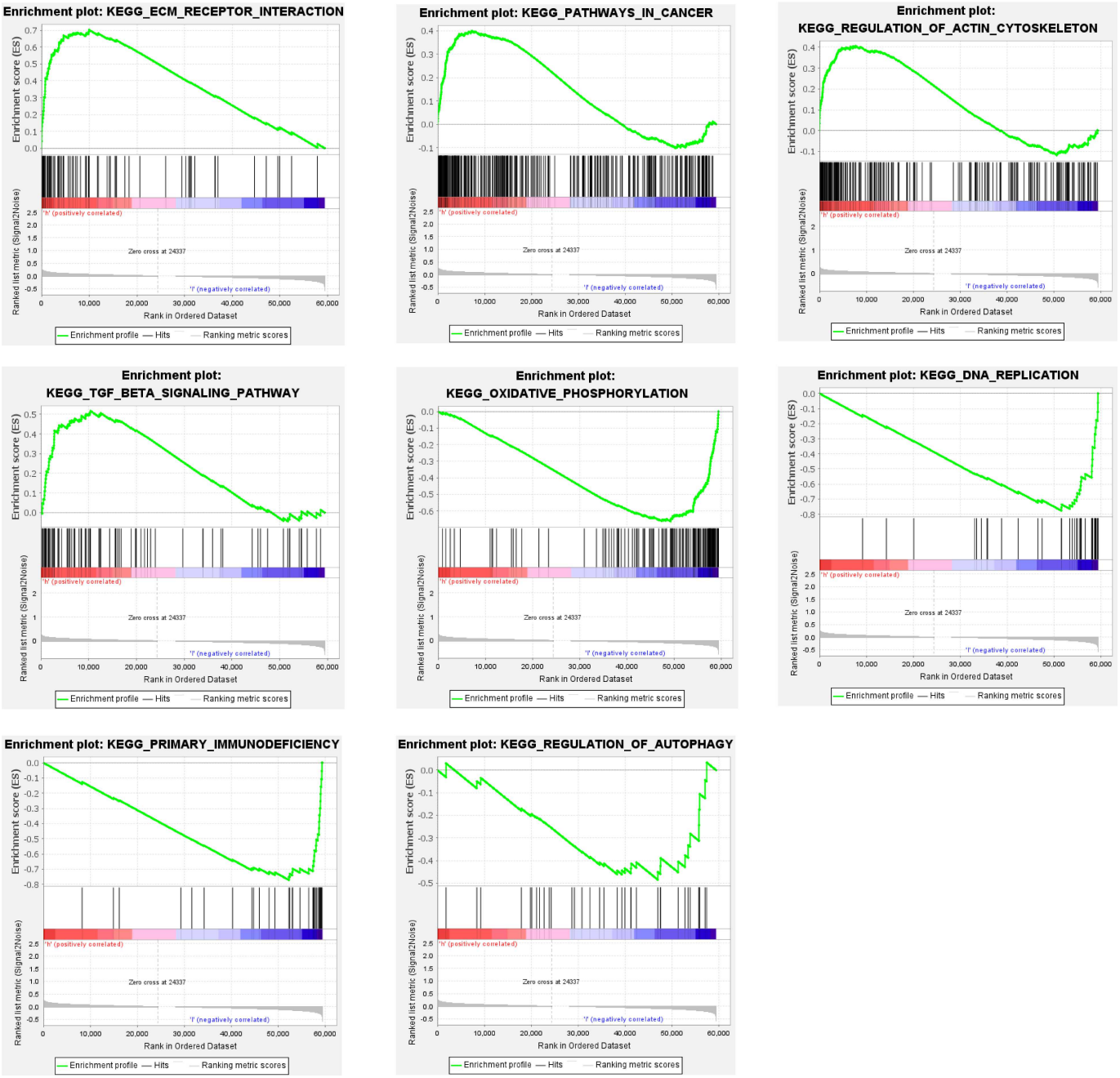

FIGURE 6. GSEA pathway enrichment analysis for the high-and low-risk groups. ECM: extracellular matrix; TGF: transforming growth factor.

was reported to play a pivotal role in its occurrence and progression [25–27]. The main treatment modalities of CESC are surgery, radiotherapy, chemotherapy and immunotherapy [28–31]. Although the OS of CESC patients has increased with advancements in treatments, many patients still develop drug resistance or tumor recurrence, leading to poor treatment outcomes [32–34]. Therefore, it is essential to delve deeper and identify potential molecular pathways, novel therapeutic targets, and biomarkers for tailored therapy and prognosis prediction of CESC patients. Ferroptosis is an iron-related cell death mechanism that has recently been the subject of fundamental scientific research and has been shown to affect tumor therapy [35–37]. Many investigations have revealed that lncRNA is related to tumor ferroptosis, cancer progression, and tumor drug resistance [38–41]. Therefore, lncRNA is anticipated to be a treatment target and biomarker for CESC.

FRLs have been found in many cancers and are reported to be associated with patient survival. Chao Mao *et al.* [42] discovered that p53-related lncRNA (*P53RRA*) is abnormally expressed in the cytoplasm and interacts with GTPase-activating protein SH3 domain-binding protein 1 (*G3BP1*) to regulate the expression of *p53*, resulting in the decrease of *p53* in the cytoplasm and the increase of *p53* in the nucleus, thus leading to cell cycle arrest, apoptosis, ferroptosis and inhibiting tumor processes. Wenjie Luo *et al.* [43] discovered that long intergenic non-protein coding RNA 1833 (*LINC01833*) was abnormally up-regulated in bladder cancer, competitively bound to *miR-129-5p* with prominin2 (*PROM2*), leading to an up-regulation of *PROM2*, which in turn induced iron output and inhibited ferroptosis

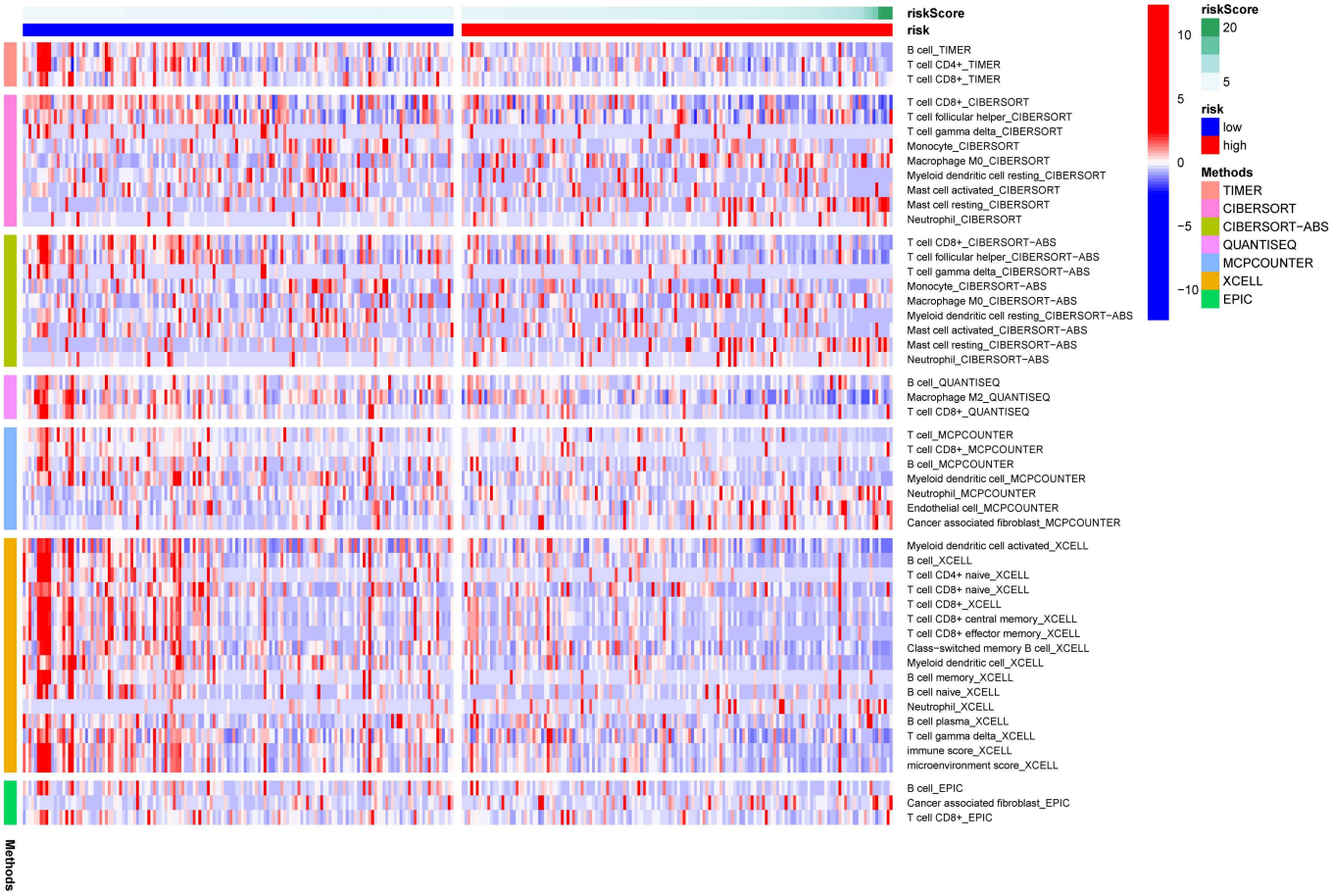

FIGURE 7. The immune heatmap showing the variations in immune cells between the high- and low-risk group.

by targeting the *PROM2*-Ferritin-multivesicular bodies (*MVBs*) pathway, thereby promoting the growth and migration capability and progression of bladder cancer cells. Hui Yang *et al.* [44] found that the hypoxia model of gastric cancer could induce CBS mRNA-destabilizing lncRNA (*CBSLR*) overexpression and form the *CBSLR*/YTH domain family protein 2 (*YTHDF2*)/cystathionine beta-synthase (*CBS*) complex, which reduced the CBS mRNA stability. In contrast, the low *CBS* expression could reduce the methylation of Acyl-CoA synthetase long-chain family 4 (*ACSL4*) protein. Furthermore, *ACSL4* degradation was accelerated, and lncRNA *CBSLR* eventually inhibited the ferroptosis process of gastric cancer in a hypoxic environment. However, there have been few investigations on ferroptosis in CESC, and the potential mechanism of ferroptosis in the CESC process has to be further investigated. In addition, the connection between FRLs and CESC has not been reported.

This is the first investigation to investigate the relationship between FRLs and CESC. After performing several data analyses, we successfully constructed the CESC predictive model using 11 FRLs (*AP003774.2*, *SOX21-AS1*, *MIAT*, *RUSC1-AS1*, *AC004847.1*, *AC009097.2*, *MIR100HG*, *AC083799.1*, *LINC00958*, *AC009065.8* and *AC131159.1*). The predictive model was found to outperform standard TMN stages in patient prognosis estimation. Furthermore, based on risk scores, patients with CESC could be separated into a high- or low-risk group. GSEA was employed to examine the differences in biological function and pathways between the two groups. The outcomes showed that the high-risk group's TGF-β signaling pathway and ECM receptor interaction were abnormally enriched. TGF-β is a multipurpose growth factor that can suppress the epithelial cell's growth [45–51]. Studies have found that the content of TGF-β in the serum changes regularly throughout the development of cervical cancer [52]. It is widely assumed that cell apoptosis occurs in response to ECM detachment [53], which is called the anoikis phenomenon [54]. Caitlin W Brown *et al.* [55] reported a correlation between the ECM pathway and ferroptosis and showed that it could physiologically trigger ferroptosis.

It has been reported that ferroptosis is strictly correlated with the tumor immune microenvironment [56–60]. Weimin Wang *et al.* [61] explored that activating CD8+ T cell increases particular lipid peroxidation in tumor cells, facilitating the process of ferroptosis. The variable expression of immunological checkpoints is critical in tumor immunotherapy [62–68]. Programmed cell death 1/programmed cell death ligand 1 (PD1/PDL1) enhances tumor resistance to immune-induced apoptosis and promotes tumor growth. Targeting the PD1/PDL1 axis can effectively inhibit tumor progression and improve patients' OS [69–78]. We found that several immune cells and immunological checkpoints were differentially expressed in the two risk subgroups after performing immune cell infiltration and immune checkpoint analyses using the CESC prognostic model. The results of drug sensitivity analysis

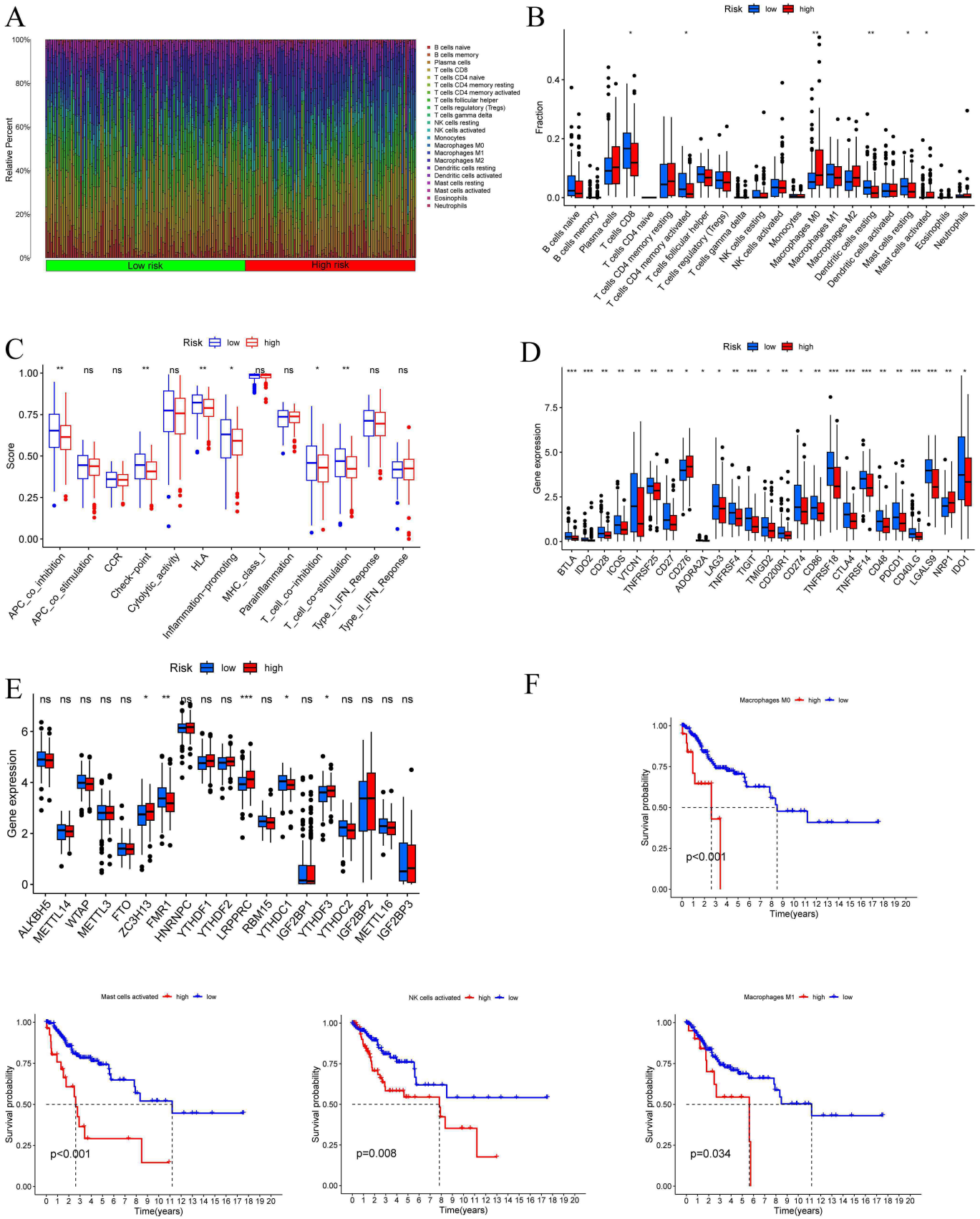

FIGURE 8. Immune-related analysis of CESC patients. (A,B) Differential analysis of immune cell infiltration between the high- and low-risk group; (C) Analysis of differences in immune function between the two studied groups; (D) Analysis of immune checkpoint differences between the two groups; (E) Analysis of variations in M6A-related genes between the two groups; (F) Survival analysis of differentially expressed immune cells in a model.

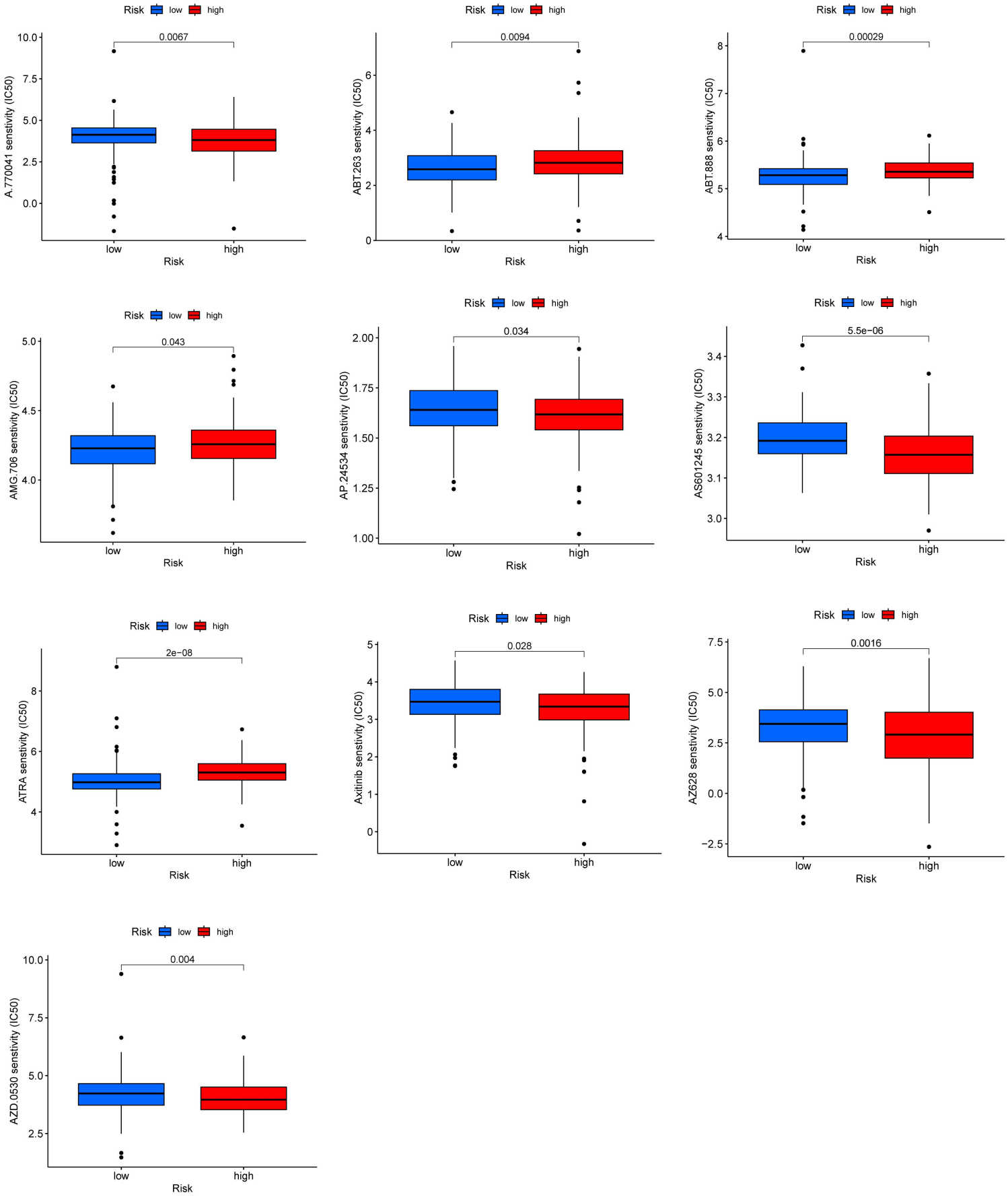

FIGURE 9. Drug sensitivity analysis showing variations in several drugs between the high- and low-risk group. IC50: inhibitory concentrations.

revealed variations in the IC50 values of several drugs between the high- and low-risk groups. Collectively, these findings might help identify patients for more efficient anti-tumor immunotherapies.

There were several limitations in this study. First, the study's findings depended only on bioinformatics analysis and lacked experimental validation. Second, we only explored the linear association between lncRNA and FRGs, thereby urging the need for in-depth mechanistic studies. Lastly, the model's accuracy was only verified in the TCGA database, and more clinical data are needed for further validation.

5. Conclusions

In summary, we constructed a prognostic model for CESC depending on 11 FRLs that had greater accuracies than other traditional clinicopathological features. We also evaluated tumor immune cell infiltration variations, immunological checkpoints and drug sensitivity across risk subgroups. Our findings offer novel insights into the role of FRLs in CESC and provide a personalized predictive tool for patient prognosis, immune response and drug therapy.

AVAILABILITY OF DATA AND MATERIALS

The datasets analysed during the current study are available in the TCGA databases (https://portal.gdc.cancer.gov/). The analyses methods and used packages are illustrated in the "Materials and methods" section. All other R code and analyses are available from the corresponding author upon request.

AUTHOR CONTRIBUTIONS

TTG and CHX—designed the research study. TTG—performed the research. JC and BW—provided help and advice on methodology, validation and resources. WW and JS—analyzed the data. TTG, CHX and JS—wrote the manuscript. All authors contributed to editorial changes in the manuscript. All authors read and approved the final manuscript.

ETHICS APPROVAL AND CONSENT TO PARTICIPATE

Not applicable.

ACKNOWLEDGMENT

Thanks to Li Jie for his help in writing the paper.

FUNDING

This research received no external funding.

CONFLICT OF INTEREST

The authors declare no conflict of interest.

SUPPLEMENTARY MATERIAL

Supplementary material associated with this article can be found, in the online version, at https://oss.ejgo.net/files/article/1735532463241740288/attachment/Supplementary%20material.zip.

REFERENCES

[1] Sung H, Ferlay J, Siegel RL, Laversanne M, Soerjomataram I, Jemal A, *et al*. Global cancer statistics 2020: GLOBOCAN estimates of incidence and mortality worldwide for 36 cancers in 185 countries. CA: A Cancer Journal for Clinicians. 2021; 71: 209–249.

[2] Siegel RL, Miller KD, Fuchs HE, Jemal A. Cancer statistics, 2022. CA: A Cancer Journal for Clinicians. 2022; 72: 7–33.

[3] Dixon SJ, Lemberg KM, Lamprecht MR, Skouta R, Zaitsev EM, Gleason CE, *et al*. Ferroptosis: an iron-dependent form of nonapoptotic cell death. Cell. 2012; 149: 1060–1072.

[4] Tang R, Hua J, Xu J, Liang C, Meng Q, Liu J, *et al*. The role of ferroptosis regulators in the prognosis, immune activity and gemcitabine resistance of pancreatic cancer. Annals of Translational Medicine. 2020; 8: 1347.

[5] Yang WS, Stockwell BR. Ferroptosis: death by lipid peroxidation. Trends in Cell Biology. 2016; 26: 165–176.

[6] Chen X, Kang R, Kroemer G, Tang D. Broadening horizons: the role of ferroptosis in cancer. Nature Reviews Clinical Oncology. 2021; 18: 280–296.

[7] Fan F, Liu P, Bao R, Chen J, Zhou M, Mo Z, *et al*. A dual PI3K/HDAC inhibitor induces immunogenic ferroptosis to potentiate cancer immune checkpoint therapy. Cancer Research. 2021; 81: 6233–6245.

[8] Chen X, Kang R, Kroemer G, Tang D. Ferroptosis in infection, inflammation, and immunity. Journal of Experimental Medicine. 2021; 218: e20210518.

[9] Dodson M, Castro-Portuguez R, Zhang DD. NRF2 plays a critical role in mitigating lipid peroxidation and ferroptosis. Redox Biology. 2019; 23: 101107.

[10] Ouyang S, Li H, Lou L, Huang Q, Zhang Z, Mo J, *et al*. Inhibition of STAT3-ferroptosis negative regulatory axis suppresses tumor growth and alleviates chemoresistance in gastric cancer. Redox Biology. 2022; 52: 102317.

[11] Wei R, Zhao Y, Wang J, Yang X, Li S, Wang Y, *et al*. Tagitinin C induces ferroptosis through PERK-Nrf2-HO-1 signaling pathway in colorectal cancer cells. International Journal of Biological Sciences. 2021; 17: 2703–2717.

[12] Shan G, Zhang H, Bi G, Bian Y, Liang J, Valeria B, *et al*. Multi-omics analysis of cancer cell lines with high/low ferroptosis scores and development of a ferroptosis-related model for multiple cancer types. Frontiers in Cell and Developmental Biology. 2021; 9: 794475.

[13] Wang W, Zhang J, Wang Y, Xu Y, Zhang S. Identifies microtubule-binding protein CSPP1 as a novel cancer biomarker associated with ferroptosis and tumor microenvironment. Computational and Structural Biotechnology Journal. 2022; 20: 3322–3335.

[14] Xing C, Yin H, Yao ZY, Xing XL. Prognostic signatures based on ferroptosis- and immune-related genes for cervical squamous cell carcinoma and endocervical adenocarcinoma. Frontiers in Oncology. 2021; 11: 774558.

[15] Djebali S, Davis CA, Merkel A, Dobin A, Lassmann T, Mortazavi A, *et al*. Landscape of transcription in human cells. Nature. 2012; 489: 101–108.

[16] Rinn JL, Chang HY. Genome regulation by long noncoding RNAs. Annual Review of Biochemistry. 2012; 81: 145–166.

[17] He T, Yuan C, Zhao C. Long intragenic non-coding RNA p53-induced transcript (LINC-PINT) as a novel prognosis indicator and therapeutic target in cancer. Biomedicine & Pharmacotherapy. 2021; 143: 112127.

[18] Kong X, Duan Y, Sang Y, Li Y, Zhang H, Liang Y, *et al*. LncRNA-CDC6 promotes breast cancer progression and function as ceRNA to target CDC6 by sponging microRNA-215. Journal of Cellular Physiology. 2019; 234: 9105–9117.

[19] Marín-Béjar O, Mas AM, González J, Martinez D, Athie A, Morales X, *et al*. The human lncRNA LINC-PINT inhibits tumor cell invasion through

a highly conserved sequence element. Genome Biology. 2017; 18: 202.

[20] Wang J, Su Z, Lu S, Fu W, Liu Z, Jiang X, *et al*. LncRNA HOXA-as2 and its molecular mechanisms in human cancer. Clinica Chimica Acta. 2018; 485: 229–233.

[21] Zhang B, Bao W, Zhang S, Chen B, Zhou X, Zhao J, *et al*. LncRNA HEPFAL accelerates ferroptosis in hepatocellular carcinoma by regulating SLC7A11 ubiquitination. Cell Death & Disease. 2022; 13: 734.

[22] Zhang Y, Luo M, Cui X, O'Connell D, Yang Y. Long noncoding RNA NEAT1 promotes ferroptosis by modulating the miR-362-3p/MIOX axis as a ceRNA. Cell Death & Differentiation. 2022; 29: 1850–1863.

[23] Miller KD, Nogueira L, Devasia T, Mariotto AB, Yabroff KR, Jemal A, *et al*. Cancer treatment and survivorship statistics, 2022. CA: A Cancer Journal for Clinicians. 2022; 72: 409–436.

[24] Siegel R, DeSantis C, Virgo K, Stein K, Mariotto A, Smith T, *et al*. Cancer treatment and survivorship statistics, 2012. CA: A Cancer Journal for Clinicians. 2012; 62: 220–241.

[25] Brisson M, Kim JJ, Canfell K, Drolet M, Gingras G, Burger EA, *et al*. Impact of HPV vaccination and cervical screening on cervical cancer elimination: a comparative modelling analysis in 78 low-income and lower-middle-income countries. The Lancet. 2020; 395: 575–590.

[26] Lin C, Slama J, Gonzalez P, Goodman MT, Xia N, Kreimer AR, *et al*. Cervical determinants of anal HPV infection and high-grade anal lesions in women: a collaborative pooled analysis. The Lancet Infectious Diseases. 2019; 19: 880–891.

[27] Malla R, Kamal MA. E6 and E7 oncoproteins: potential targets of cervical cancer. Current Medicinal Chemistry. 2021; 28: 8163–8181.

[28] Colli LM, Machiela MJ, Zhang H, Myers TA, Jessop L, Delattre O, *et al*. Landscape of combination immunotherapy and targeted therapy to improve cancer management. Cancer Research. 2017; 77: 3666–3671.

[29] Lee YT, Tan YJ, Oon CE. Molecular targeted therapy: treating cancer with specificity. European Journal of Pharmacology. 2018; 834: 188–196.

[30] Li H, Wu X, Cheng X. Advances in diagnosis and treatment of metastatic cervical cancer. Journal of Gynecologic Oncology. 2016; 27: e34.

[31] Mun EJ, Babiker HM, Weinberg U, Kirson ED, Von Hoff DD. Tumor-treating fields: a fourth modality in cancer treatment. Clinical Cancer Research. 2018; 24: 266–275.

[32] Bhattacharya B, Mohd Omar MF, Soong R. The Warburg effect and drug resistance. British Journal of Pharmacology. 2016; 173: 970–979.

[33] Friedmann Angeli JP, Krysko DV, Conrad M. Ferroptosis at the crossroads of cancer-acquired drug resistance and immune evasion. Nature Reviews Cancer. 2019; 19: 405–414.

[34] Vasan N, Baselga J, Hyman DM. A view on drug resistance in cancer. Nature. 2019; 575: 299–309.

[35] Koren E, Fuchs Y. Modes of regulated cell death in cancer. Cancer Discovery. 2021; 11: 245–265.

[36] Liu P, Wang W, Li Z, Li Y, Yu X, Tu J, *et al*. Ferroptosis: a new regulatory mechanism in osteoporosis. Oxidative Medicine and Cellular Longevity. 2022; 2022: 1–10.

[37] Gao W, Wang X, Zhou Y, Wang X, Yu Y. Autophagy, ferroptosis, pyroptosis, and necroptosis in tumor immunotherapy. Signal Transduction and Targeted Therapy. 2022; 7: 196.

[38] Chen Q, Wang W, Wu Z, Chen S, Chen X, Zhuang S, *et al*. Over-expression of lncRNA TMEM161B-AS1 promotes the malignant biological behavior of glioma cells and the resistance to temozolomide *via* up-regulating the expression of multiple ferroptosis-related genes by sponging hsa-miR-27a-3p. Cell Death Discovery. 2021; 7: 311.

[39] Fu H, Zhang Z, Li D, Lv Q, Chen S, Zhang Z, *et al*. LncRNA *PELATON*, a ferroptosis suppressor and prognositic signature for GBM. Frontiers in Oncology. 2022; 12: 817737.

[40] Huang G, Xiang Z, Wu H, He Q, Dou R, Lin Z, *et al*. The lncRNA BDNF-as/WDR5/FBXW7 axis mediates ferroptosis in gastric cancer peritoneal metastasis by regulating VDAC3 ubiquitination. International Journal of Biological Sciences. 2022; 18: 1415–1433.

[41] Ni T, Huang X, Pan S, Lu Z. Inhibition of the long non-coding RNA ZFAS1 attenuates ferroptosis by sponging miR-150-5p and activates CCND2 against diabetic cardiomyopathy. Journal of Cellular and Molecular Medicine. 2021; 25: 9995–10007.

[42] Mao C, Wang X, Liu Y, Wang M, Yan B, Jiang Y, *et al*. A G3BP1-interacting lncRNA promotes ferroptosis and apoptosis in cancer *via* nuclear sequestration of p53. Cancer Research. 2018; 78: 3484–3496.

[43] Luo W, Wang J, Xu W, Ma C, Wan F, Huang Y, *et al*. LncRNA RP11-89 facilitates tumorigenesis and ferroptosis resistance through PROM2-activated iron export by sponging miR-129-5p in bladder cancer. Cell Death & Disease. 2021; 12: 1043.

[44] Yang H, Hu Y, Weng M, Liu X, Wan P, Hu Y, *et al*. Hypoxia inducible lncRNA-CBSLR modulates ferroptosis through m6a-YTHDF2-dependent modulation of CBS in gastric cancer. Journal of Advanced Research. 2022; 37: 91–106.

[45] Derynck R, Muthusamy BP, Saeteurn KY. Signaling pathway cooperation in TGF-β-induced epithelial-mesenchymal transition. Current Opinion in Cell Biology. 2014; 31: 56–66.

[46] Hartsough MT, Mulder KM. Transforming growth factor-beta signaling in epithelial cells. Pharmacology & Therapeutics. 1997; 75: 21–41.

[47] Katsuno Y, Derynck R. Epithelial plasticity, epithelial-mesenchymal transition, and the TGF-β family. Developmental Cell. 2021; 56: 726–746.

[48] Sharkey DJ, Macpherson AM, Tremellen KP, Mottershead DG, Gilchrist RB, Robertson SA. TGF-β mediates proinflammatory seminal fluid signaling in human cervical epithelial cells. The Journal of Immunology. 2012; 189: 1024–1035.

[49] Xu J, Lamouille S, Derynck R. TGF-beta-induced epithelial to mesenchymal transition. Cell Research. 2009; 19: 156–172.

[50] Yue J, Mulder KM. Transforming growth factor-beta signal transduction in epithelial cells. Pharmacology & Therapeutics. 2001; 91: 1–34.

[51] Zavadil J, Böttinger EP. TGF-beta and epithelial-to-mesenchymal transitions. Oncogene. 2005; 24: 5764–5774.

[52] Wu HS, Li YF, Chou CI, Yuan CC, Hung MW, Tsai LC. The concentration of serum transforming growth factor beta-1 (TGF-beta1) is decreased in cervical carcinoma patients. Cancer Investigation. 2002; 20: 55–59.

[53] Meredith JE, Fazeli B, Schwartz MA. The extracellular matrix as a cell survival factor. Molecular Biology of the Cell. 1993; 4: 953–961.

[54] Frisch S, Francis H. Disruption of epithelial cell-matrix interactions induces apoptosis. Journal of Cell Biology. 1994; 124: 619–626.

[55] Brown CW, Amante JJ, Goel HL, Mercurio AM. The α6β4 integrin promotes resistance to ferroptosis. Journal of Cell Biology. 2017; 216: 4287–4297.

[56] Gong C, Ji Q, Wu M, Tu Z, Lei K, Luo M, *et al*. Ferroptosis in tumor immunity and therapy. Journal of Cellular and Molecular Medicine. 2022; 26: 5565–5579.

[57] Jiang X, Stockwell BR, Conrad M. Ferroptosis: mechanisms, biology and role in disease. Nature Reviews Molecular Cell Biology. 2021; 22: 266–282.

[58] Tang R, Xu J, Zhang B, Liu J, Liang C, Hua J, *et al*. Ferroptosis, necroptosis, and pyroptosis in anticancer immunity. Journal of Hematology & Oncology. 2020; 13: 110.

[59] Wiernicki B, Maschalidi S, Pinney J, Adjemian S, Vanden Berghe T, Ravichandran KS, *et al*. Cancer cells dying from ferroptosis impede dendritic cell-mediated anti-tumor immunity. Nature Communications. 2022; 13: 3676.

[60] Xu H, Ye D, Ren M, Zhang H, Bi F. Ferroptosis in the tumor microenvironment: perspectives for immunotherapy. Trends in Molecular Medicine. 2021; 27: 856–867.

[61] Wang W, Green M, Choi JE, Gijón M, Kennedy PD, Johnson JK, *et al*. CD8+ T cells regulate tumour ferroptosis during cancer immunotherapy. Nature. 2019; 569: 270–274.

[62] Franzin R, Netti GS, Spadaccino F, Porta C, Gesualdo L, Stallone G, *et al*. The use of immune checkpoint inhibitors in oncology and the occurrence of AKI: where do we stand? Frontiers in Immunology. 2020; 11: 574271.

[63] Galluzzi L, Humeau J, Buqué A, Zitvogel L, Kroemer G. Immunostimulation with chemotherapy in the era of immune checkpoint inhibitors. Nature Reviews Clinical Oncology. 2020; 17: 725–741.

[64] Heinhuis KM, Ros W, Kok M, Steeghs N, Beijnen JH, Schellens JHM. Enhancing antitumor response by combining immune checkpoint inhibitors with chemotherapy in solid tumors. Annals of Oncology. 2019; 30: 219–235.

[65] Kalbasi A, Ribas A. Tumour-intrinsic resistance to immune checkpoint blockade. Nature Reviews Immunology. 2020; 20: 25–39.

[66] Miller JFAP, Sadelain M. The journey from discoveries in fundamental immunology to cancer immunotherapy. Cancer Cell. 2015; 27: 439–449.

[67] Ho P, Kaech SM. Reenergizing T cell anti-tumor immunity by harnessing immunometabolic checkpoints and machineries. Current Opinion in Immunology. 2017; 46: 38–44.

[68] Hosseinkhani N, Derakhshani A, Kooshkaki O, Abdoli Shadbad M, Hajiasgharzadeh K, Baghbanzadeh A, *et al*. Immune checkpoints and CAR-T cells: the pioneers in future cancer therapies? International Journal of Molecular Sciences. 2020; 21: 8305.

[69] Lei Q, Wang D, Sun K, Wang L, Zhang Y. Resistance mechanisms of anti-PD1/PDL1 therapy in solid tumors. Frontiers in Cell and Developmental Biology. 2020; 8: 672.

[70] Brahmer JR, Tykodi SS, Chow LQM, Hwu W, Topalian SL, Hwu P, *et al*. Safety and activity of anti-PD-L1 antibody in patients with advanced cancer. The New England Journal of Medicine. 2012; 366: 2455–2465.

[71] Daassi D, Mahoney KM, Freeman GJ. The importance of exosomal PDL1 in tumour immune evasion. Nature Reviews Immunology. 2020; 20: 209–215.

[72] Gou Q, Dong C, Xu H, Khan B, Jin J, Liu Q, *et al*. PD-L1 degradation pathway and immunotherapy for cancer. Cell Death & Disease. 2020; 11: 955.

[73] Jiang Q, Huang J, Zhang B, Li X, Chen X, Cui B, *et al*. Efficacy and safety of anti-PD1/PDL1 in advanced biliary tract cancer: a systematic review and meta-analysis. Frontiers in Immunology. 2022; 13: 801909.

[74] Jin Y, Wei J, Weng Y, Feng J, Xu Z, Wang P, *et al*. Adjuvant therapy with PD1/PDL1 inhibitors for human cancers: a systematic review and meta-analysis. Frontiers in Oncology. 2022; 12: 732814.

[75] Liu J, Chen Z, Li Y, Zhao W, Wu J, Zhang Z. PD-1/PD-L1 checkpoint inhibitors in tumor immunotherapy. Frontiers in Pharmacology. 2021; 12: 731798.

[76] Marchetti A, Di Lorito A, Buttitta F. Why anti-PD1/PDL1 therapy is so effective? Another piece in the puzzle. Journal of Thoracic Disease. 2017; 9: 4863–4866.

[77] Patel JJ, Levy DA, Nguyen SA, Knochelmann HM, Day TA. Impact of PD-L1 expression and human papillomavirus status in anti-PD1/PDL1 immunotherapy for head and neck squamous cell carcinoma-systematic review and meta-analysis. Head & Neck. 2020; 42: 774–786.

[78] Stenehjem DD, Tran D, Nkrumah MA, Gupta S. PD1/PDL1 inhibitors for the treatment of advanced urothelial bladder cancer. OncoTargets and Therapy. 2018; 11: 5973–5989.

How to cite this article: Tingting Gu, Caihong Xu, Jing Chen, Bin Wan, Wei Wang, Jun Shi. Construction of a ferroptosis-related lncRNA signature for predicting prognosis, immune response and drug sensitivity in cervical squamous cell carcinoma and endocervical adenocarcinoma. European Journal of Gynaecological Oncology. 2023; 44(6): 29-42. doi: 10.22514/ejgo.2023.096.